

---

# Learning Real-World Robot Policies by Dreaming

---

AJ Piergiovanni      Alan Wu      Michael S. Ryoo  
 School of Informatics, Computing, and Engineering  
 Indiana University Bloomington  
 {ajpiergi, alanwu, mryoo}@indiana.edu

## Abstract

Learning to control robots directly based on images is a primary challenge in robotics. However, many existing reinforcement learning approaches require iteratively obtaining millions of samples to learn a policy which can take significant time. In this paper, we focus on the problem of learning real-world robot action policies solely based on a few random off-policy samples. We learn a realistic *dreaming model* that can emulate samples equivalent to a sequence of images from the actual environment, and make the agent learn action policies by interacting with the dreaming model rather than the real world. We experimentally confirm that our dreaming model can learn realistic policies that transfer to the real-world.

## 1 Introduction

Learning to control robots directly based on its camera input (i.e., images) has been one of the primary challenges in robotics. Recently, a significant amount of progress has been made in deep reinforcement learning (RL), learning control policies using raw image data from physics engines and computer game environments [12, 21]. These methods have also been applied to real-world robots, obtaining promising results [6, 34]. The concept of learning state representations with convolutional neural networks (CNNs) instead of using hand-crafted states particularly benefits robots, which are required to process high dimensional image data with rich scene information.

However, many of these reinforcement learning methods require obtaining millions of samples (i.e., trajectories) over multiple training iterations to converge to an optimal policy. This is often very expensive for real-world robots; obtaining each sample of a robot trial may take multiple minutes even with a well-prepared setup, resulting in the total robot learning time to be weeks/months every time the setting changes or a new task is needed (e.g., 3000 robot hours in [18] and 700 hours in [25]). Further, there are also safety issues when obtaining real-world robot samples. This difficulty is one of the reasons why deep reinforcement learning works applied to simulators (e.g., MuJoCo) or computer games (e.g., Atari) have been much more common, in contrast to real-world robots.

In this paper, we focus on the problem of learning real-world robot action policies solely based on relatively few random off-policy initial samples. The main idea is to learn a realistic *dreaming model* that can emulate samples equivalent to sequences of image frames from the actual environment, and make the agent (i.e., a robot) learn action policies by interacting with the dreaming model instead of the real-world. Our dreaming model is explicitly designed to learn a good state representation space that allows the generation of realistic samples from scratch while also correctly modeling their dynamics over a series of actions. The objective is to make the dreaming model synthesize real-world robot experience by generating ‘dreamed trajectories/samples’ composed of state-action pairs that correspond to realistic image frames. Such capability allows the robot to learn its action policy by interacting with the dreaming model, even without any real-world robot interactions, iteratively visiting states within the dream. This is not only important for making the policy learning much more efficient by minimizing real robot executions, but also is crucial for the situations where robot interactions with its real-world environment is expensive and prohibited.

We introduce a fully convolutional network architecture combining a variational autoencoder and an action-conditioned future regressor to implement our dreaming model. The use of the dreaming model can be viewed as an extension of previous model-based reinforcement learning works using ‘imagined trajectories’ in addition to real trajectories [12, 29, 36]. The main difference is that (i) our state representation space is learned in a way that it is optimized for generating dreamed trajectories from scratch while being realistic. The state space our dreaming model learns is explicitly trained to make any of its samples correspond to a realistic video frame, and this allows generation of dreamed trajectories with random start states unlike prior works. Further, (ii) our proposed approach attempts to learn such realistic model from random initial trajectories, different from previous works. Making a reinforcement learning agent interact with our learned dreaming model and optimizing its policy solely based on it may also be interpreted as zero-real-trial reinforcement learning, and (iii) we confirm such capability experimentally with a real-world robot receiving real-world image frames.

Our experiments were conducted with a real-time robot in a real-world office environment. We show that learning our dreaming model based on initial random robot samples is possible, and confirm that it allows multiple different reinforcement learning algorithms to obtain real robot action policies by dreaming. We also experimentally confirm that our dreaming model can be extended to learn a policy that could handle ‘unseen’ object targets (i.e., zero-sample object target transfer) by learning a general state representation space shared across multiple objects.

## 2 Related works

Convolutional neural networks (CNNs) have been greatly successful on many traditional computer vision tasks. These include image classification [15, 28], object detection [8, 19] and activity recognition in videos [1, 24]. Learning features and representations optimized for the training data using CNNs enabled better recognition in these tasks.

Several works studied using CNNs for reinforcement learning of policies, designing deep reinforcement learning models. These works learn state representations from raw images, and allow control of the agents directly based on image inputs [7, 12, 14, 21, 37]. Zhang et al. [37] showed that policy learning of a robot is possible with synthetic images but found that the learned policy does not work well when directly applied to real-world images. Finn et al. [7] trained an autoencoder to learn state representations to be used for reinforcement policy learning of real-world robots.

There also are model-based reinforcement learning works with state-transition models [6, 17, 35]. PILCO [3, 20] uses a Gaussian process (GP) to model the state-transition model and samples many trajectories from it to train a policy. However, this method is only applied to small, hand-crafted state spaces, as using GPs with complex real-world images is not computationally feasible/easy. Finn et al. [5] learned a LSTM model to predict future video frames based on actions, which was applied to the planning-based robot control [6]. However, it focused on the model predictive control (MPC) and was not about learning the policy function, analogous to [34].

Combining model-free reinforcement learning with model-based methods has also been studied. They often learn the state-transition model (as a neural network) and use the model to initialize/benefit the learning of model-free policies [22, 26]. This is also relevant to the use of ‘imagined trajectories’ generated by applying the state-transition model to states from on-policy real-world trials. This includes Dyna [29] as well as more recent works [9, 27, 33]. There are also works using state-transition models to combine reinforcement learning with planning, such as VPN [23] and I2A [36].

Other works have explored transferring policies learned in simulated environments to real environments for robots [2, 30, 32]; however, these environment simulators are hand-crafted rather than learned from data. Our dreaming model may be viewed as ‘learning’ a simulator capturing real-world scene changes and learning realistic policies using the learned simulator. The main difference between our work and the use of simulators for robot learning (e.g., [31]) is that such (hand-crafted) simulator is not given in our case but needs to be learned from random initial samples.

## 3 Background

We follow the standard reinforcement learning setting and formulate policy learning as learning in a Markov decision process (MDP). The MDP,  $(\mathcal{S}, \mathcal{A}, f, r)$  consists of a state space,  $\mathcal{S}$  and an action space  $\mathcal{A}$ .  $f$  is the state transition function  $f : \mathcal{S} \times \mathcal{A} \mapsto \mathcal{S}$ , which maps from a starting state  $s_t$  and

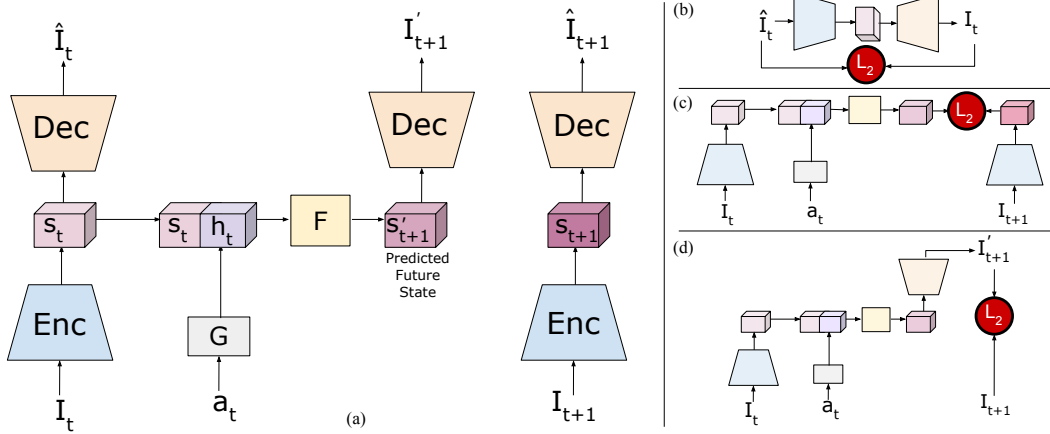


Figure 1: Illustration of our dreaming model. **(a)** The encoder, action representation, future regressor and decoder modules. **(b)** Image reconstruction loss for the autoencoder. **(c)**  $L_2$  loss for the future regressor. **(d)** Future image reconstruction loss for the future image prediction. Rectangles in the figure are the CNN layers, and 3-D cuboids are the representations. Circles indicate losses.

action  $a_t$  to an ending state  $s_{t+1}$ . After each action, the environment gives a reward,  $\mathcal{R} : \mathcal{S} \mapsto r$ . We denote a trajectory (i.e., a sequence of states and actions) as  $\tau = (s_0, a_0, s_1, a_1, \dots, s_T)$  and we obtain a trajectory  $\tau = \rho(\pi)$  by sampling from a stochastic policy providing the actions:  $\pi(a_t|s_t)$ . The objective of reinforcement learning is to learn the policy maximizing the expected total ( $\gamma$ -discounted) reward from the start distribution,  $J(\pi) = \mathbb{E}_{(s_t, a_t) \sim \rho(\pi)} [\sum_{i=0}^T \gamma^i \mathcal{R}(s_i)]$ .

In this work, we consider continuous state and action spaces. We particularly take advantage of policy gradient methods including an actor-critic that learns an action-value  $Q$  function  $Q_\pi(s_t, a_t) = \mathbb{E}_{(s_t, a_t) \sim \rho(\pi)} [\sum_{i=t}^T \gamma^{i-t} \mathcal{R}(s_i)]$  together with the actor network  $\pi(a_t|s_t)$ . Our agent (i.e., a robot) in a real-world environment receives an image input  $I_t$  at every time step  $t$ , and we learn the function from  $I_t$  to the state representation  $s_t$  together with its policy. These functions are implemented in terms of CNNs, as was done in previous deep reinforcement learning works.

## 4 Dreaming model

Our dreaming model is a combination of a convolutional autoencoder and a action-conditioned future representation regressor. It enables encoding of an image frame (i.e., robot observation) into the representation abstracting scene (i.e., robot state), and allows predicting the expected future representation given any state and a robot action to take (i.e., transition).

More specifically, our dreaming model consists of the following four function components, governed by the learned parameters  $\theta_{Enc}$ ,  $\theta_{Dec}$ ,  $\theta_f$ , and  $\theta_R$ :

**State Encoder**  $Enc_\theta : I \mapsto s$

**State Decoder**  $Dec_\theta : s \mapsto I$

**State-transition**  $f_\theta : s_t, a_t \mapsto s_{t+1}$

**Reward/End Detector**  $R_\theta : s \mapsto r$

$I_t = Dec(s_t = Enc(I_t))$  is a variational autoencoder that learns a compact scene representation, to be used as the state:  $s_t$ .  $s_{t+1} = f(s_t, a_t)$  is a state transition model which is also often described as ‘future representation regression’ in computer vision.  $r_t = R(s_t)$  is a CNN trained to predict the immediate reward corresponding to the state  $s_t$ . Note that this reward is often sparse, being constant in all states other than a terminal state. All these functions are fully convolutional neural networks.

The important properties of our dreaming model are that (1) its state space is learned to make decoding of current/future robot states back to real-world image frames possible and that (2) the space is explicitly trained to make sense even when we randomly sample states from it. Having such realistic model enables our robot to learn its action policy by generating ‘dreamed trajectories’ from any random starting states/images, unlike prior works using imagined trajectories.

The full model is shown in Fig. 1, together with the description of our losses to train the entire dreaming model. Note that none of our losses are dependent on the policy to be learned: we are able to learn the dreaming model from trajectories of a random initial policy.

---

**Algorithm 1** Actor-Critic policy learning in a dream
 

---

```

function ACTOR-CRITIC( $f, R$ )
  Initialize policy  $\pi_\theta$ , value function  $V_\phi$ 
  for  $i = 0$  to num episodes do
    Get random starting state,  $s_0 \sim \mathcal{N}(0, 1)$ 
    for  $t = 0$  to  $T$  do
       $a_t \sim \pi_\theta(a_t | s_t)$ 
       $s_{t+1} = f(s_t, a_t)$ 
       $y = R(s_t) + \gamma V_\phi(s_{t+1})$ 
       $\hat{A} = y - V_\phi(s_t)$ 
       $\nabla_\theta J(\theta) \approx \nabla_\theta \log \pi_\theta(a_t | s_t) \hat{A}$ 
       $\theta = \theta + \alpha \nabla_\theta J(\theta)$ 
       $\phi = \phi + \nabla_\phi |V_\phi(s_t) - y|$ 
    end for
  end for
end function
  
```

---

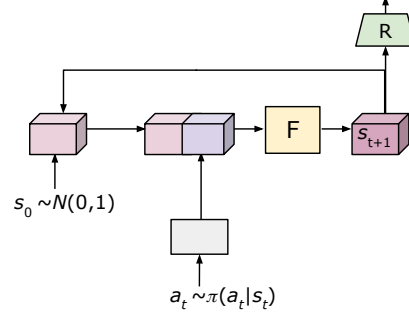


Figure 2: Illustration of how our dreaming works for the policy learning. A random start state is sampled and then actions are sampled from the policy. The state-transition model predicts the next state. This process is repeated until the end detector signals the end of the trial.

#### 4.1 Learning state representation

We learn a state representation based on a variational autoencoder (VAE) [13] which takes an image as input and learns a latent state representation optimized to reconstruct the given image. Unlike previous works using VAEs, we maintain spatial information by designing/using a ‘convolutional’ VAE, where our latent representation is a  $W \times H \times C$  tensor rather than a  $C$ -dimensional vector in traditional VAEs. Here,  $W$  is the spatial width of the representation,  $H$  is the height, and  $C$  is the number of channels. VAEs assume a prior distribution over the latent space  $s \sim \mathcal{N}(0, 1)$  and minimize the KL-divergence between the latent encoded representation,  $Enc(I) \sim q(s|I)$  and the prior. This is an important property allowing us to randomly sample the latent space  $s \sim \mathcal{N}(0, 1)$  to obtain a new state that corresponds to a realistic image, once learned. The encoder outputs  $\mu, \sigma = Enc(I)$  and we sample from  $s \sim \mathcal{N}(\mu, \sigma)$  to obtain the state representation during the training. Once the training of the autoencoder is done, we set  $s = \mu$ .

Given the encoder CNN  $Enc$  and decoder CNN  $Dec$ , we minimize the following loss (Fig. 1 (b)):

$$\mathcal{L}_{VAE} = ||Dec(Enc(I)) - I||_2 + D_{KL}(q(s|I)||p(s)) \quad (1)$$

The state representation model is responsible for abstracting the important scene information into a small, latent state representation.

#### 4.2 Learning the state-transition model

We learn a state-transition model by extending the future regression formulation from [16] to become action-conditioned. Our state-transition model takes the current state,  $s_t$ , and action,  $a_t$ , as input and outputs the next state,  $s_{t+1}$ . Since our state representation is convolutional, we train a CNN,  $G$  to transform the action also into a convolutional representation by using a fully connected layer followed by depooling to create a  $W \times H \times C'$  representation, followed by several convolution layers to learn a convolutional action representation. We concatenate the action representation with the state along the channel axis and use several convolutional layers to predict the next state:

$$s_{t+1} = f(s_t, a_t) = F([s_t, G(a_t)]) \quad (2)$$

We combine the state-transition model with the state representation model to obtain the predicted future image:  $\hat{I}_{t+1} = Dec(f(Enc(I_t), a_t))$ . We can then minimize the following loss:

$$\mathcal{L}_f = ||f(Enc(I_t), a_t) - Enc(I_{t+1})||_2 + ||Dec(f(Enc(I_t), a_t)) - I_{t+1}||_2 \quad (3)$$

which learns to minimize the difference between the the future-regressed state and the true future state and the difference between the true next image and predicted future image. This is the combination of Fig. 1 (c) and (d).

We jointly train the state-transition model and the representation by minimizing the following loss:

$$\mathcal{L} = \mathcal{L}_{VAE} + \lambda \mathcal{L}_f \quad (4)$$

where  $\lambda = 0.5$  and weights the losses. This combines the losses described in Fig. 1 (b), (c), and (d).

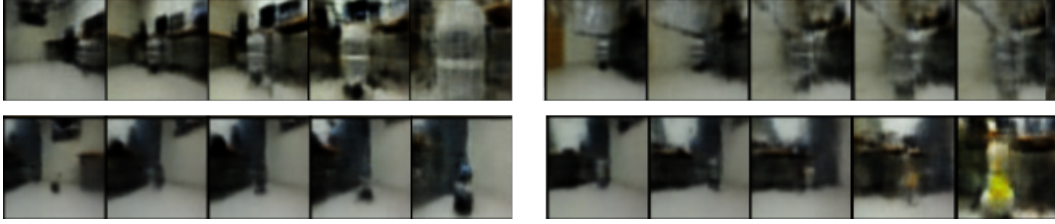


Figure 3: Four dreamed trajectory examples from random start states. For instance, approaching the air filter object is dreamed in the top-left example. Leftmost images are the (decoded) randomly generated start states. Although the images look realistic, none of these are from real robot samples.

## 5 Policy learning in a dream

Given the learned state representation space,  $\mathcal{S}$ , trained state-transition model,  $f$ , and sparse reward/end detector CNN,  $R$ , we can learn a policy,  $\pi$ , to maximize the expected reward using any reinforcement learning algorithm. Since our state representation is learned using a variational autoencoder, we are able to start a trajectory from an unseen state by randomly sampling (i.e., generating) from the prior,  $s_0 \sim \mathcal{N}(0, 1)$ . We then obtain a ‘dreamed’ trajectory  $\tau = (s_0, a_0 \sim \pi(a_0|s_0), s_1 = f(s_0, a_0), a_1 \sim \pi(a_1|s_1), s_2 = f(s_1, a_1), \dots)$  by following our action policy and transition model. We compute the discounted reward for the dreamed trajectory as  $\sum_{t=0}^T \gamma^{T-t} R(s_t)$ , and update the policy being learned accordingly. Note that we can also start from seen states using the decoder and an image to obtain  $s_0 = \text{Enc}(I)$  where  $I$  is from the real robot sample.

In Algorithm 1, we show an example of actor-critic policy learning in a dream. This allows the agent to ‘dream’ unseen starting states and explore the environment without any real-world trials. Our approach is able to benefit any reinforcement policy learning methods in general, and we are showing an actor-critic method as an example. Fig. 2 illustrates how our model generates dreamed episodes.

## 6 Experiments

### 6.1 Environment

We use a complex real-world office room as our environment and have a ground mobility robot, TurtleBot 2, interacting with a target object. Our environment consists of 7 different target objects such as a volleyball, shopping bag, and backpack. The robot only obtains its camera input, which is the first-person view of the room.

We represent actions of our ground mobility robot in polar coordinates,  $a_t = (\Delta\alpha, \Delta v, \Delta\omega)$ , where  $\Delta\alpha$  controls the initial rotation,  $\Delta v$  determines how much to move and  $\Delta\omega$  determines the final rotation. We constrain the continuous action space so that  $\Delta\alpha, \Delta\omega \in [-30, 30]^\circ$  and  $\Delta v \in [0, 20]\text{cm}$ .

To train the dreaming model, we collect a dataset consisting of 40,000 images. We allow the robot to take random actions in the environment and we store the starting image, action and resulting image pairs as  $(I_t, a_t, I_{t+1})$ . We use this data to train our dreaming model: the autoencoder and future regression model. We then annotated the images corresponding to the goal state to train the reward/end detector CNN. This CNN determines when the goal state is reached.

We emphasize once more that no real robot samples were provided except random policy initial samples in all our experiments.

### 6.2 Baselines and dreaming models

In order to confirm the effectiveness of our dreaming model (which is the combination of the jointly learned convolutional representation encoder and state-transition model), we implemented several baseline models that can also generate imagined trajectories as well as our dreaming models.

We implemented the traditional (i.e., standard) approach of learning a state-transition model on top of the linear CNN-based state representations, as was done in [12, 23, 36]. Linear CNN-based state representations has been widely used (e.g., [21]), and the above works learn such representations



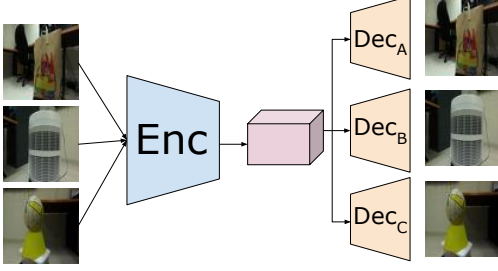


Figure 4: Shared encoder with target specific decoders (TSD). This architecture forces the learned state representation to contain no information specific to the visible target.

Table 1: Normalized  $L_1$  distances (Eq. 5) between actual vs. predicted future state.

|                   | Relative ( $D_1$ ) | Mean ( $D_2$ ) |
|-------------------|--------------------|----------------|
| Standard-ImageNet | 0.98               | 0.741          |
| Standard-Reward   | 0.97               | 0.729          |
| Dreaming (Linear) | 0.82               | 0.558          |
| Dreaming (Conv.)  | 0.71               | 0.448          |
| Dreaming (TSD)    | 0.68               | 0.412          |

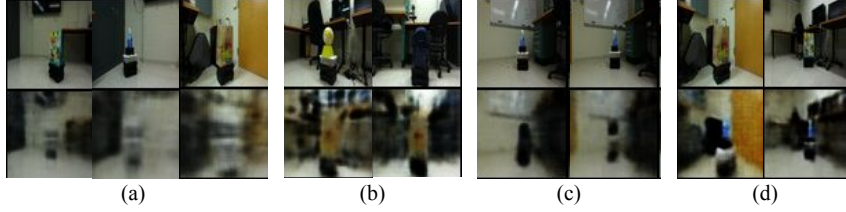


Figure 5: Example of reconstructing unseen targets. Turning (a) bags and a bottle into an airfilter; (b) a volleyball and a backpack into a bag; (c) a bottle into a backpack; and (d) a bag into a bottle.

jointly with the state-transition model. These approaches do not use a decoder and are usually trained using on-policy trials. To obtain a state representation based on these approaches in our scenario of only using random initial trajectories for the learning, we compare two different variations: (1) a CNN initialized with ImageNet [4] training, and (2) a CNN trained to detect the goal state. In both these baselines, we use the output from the final fully connected layer before the classification as the state representation. We also implemented (3) a version of our dreaming model using a variational autoencoder to learn a ‘linear’ state representation similar to [10]. Finally, we implemented (4) the full version of our dreaming model with convolutional state and action representations. We describe our architectures and training details in Appendix A (in the supplementary material).

**Evaluating accuracies of the learned dreaming models:** As our initial experiment, we directly compare the normalized  $L_1$  distance (Eq. 5) between predicted vs. actual future state representations in Table 1. This captures the relative difference between the future predicted state and the true future state. The (normalized) distance metrics we used are as follows:

$$D_1(s_t, a_t, s_{t+1}, f) = \frac{f(s_t, a_t) - s_{t+1}}{s_t - s_{t+1}}, \quad D_2(s_t, a_t, s_{t+1}, f) = \frac{f(s_t, a_t) - s_{t+1}}{\frac{1}{N} \sum (s_i - s_j)}, \forall i, j \quad (5)$$

We find that the use of a decoder in our dreaming model greatly improves the accuracy over the conventional models. We also confirm that using our convolutional state/action representation design provides the best accuracy.

**Learning shared state-representation:** In a scenario where we have many different target objects but want to learn a generic policy applicable to all the objects, we can extend our dreaming model by training an autoencoder using target specific decoders (TSD). Using a single decoder (shared by all images/objects) requires the state representation to maintain certain information about object appearances or types, in order for the decoder to reconstruct it. On the other hand, if we use a target specific decoder, we are able to encourage the representation to contain no object-dependent information, making the target-specific-decoder responsible for reconstructing the object appearance (Fig. 4). Having such encoder allows for better policy learning as the policy does not depend on which object is present in our scenarios. This has the effect of reducing the size of the state space. Table 1 confirms that this representation benefits the overall learning.

Additionally, the use of such architecture allows us to recognize unseen target objects. We can apply the encoder to an image containing an unseen target object, then apply one of the decoders to the representation to reconstruct the scene with the other target. Examples of this are shown in Fig. 5. We confirm this further in Subsection 6.5 where we force the robot to interact with unseen objects.

Table 2: Offline evaluation of the target ‘approach’ task. We test our dreaming models using various reinforcement learning algorithms, averaged over 500 trials.

|                  | Standard |      |          | Dreaming (linear) |      |          | Dreaming (conv) |      |          |
|------------------|----------|------|----------|-------------------|------|----------|-----------------|------|----------|
|                  | Random   | Real | Combined | Random            | Real | Combined | Random          | Real | Combined |
| Constant Forward | 22%      |      |          |                   |      |          |                 |      |          |
| MPC [22]         | -        | 24%  | -        | -                 | 28%  | -        | -               | 28%  | -        |
| REINFORCE        | 25%      | 26%  | 26%      | 26%               | 44%  | 39%      | 54%             | 50%  | 55%      |
| Actor-Critic     | 25%      | 26%  | 26%      | 34%               | 34%  | 34%      | 55%             | 52%  | 61%      |
| CMA-ES [11]      | 26%      | 27%  | 25%      | 32%               | 36%  | 35%      | 57%             | 54%  | 62%      |

Table 3: Offline evaluation of the target approach/avoid tasks. We report the percentage of successful trials, based on the policies learned with Actor-Critic. We also measure the robot’s average distance from the target in the avoidance task.

|                   | Approach | Avoid (Success) | Avoid (Dist) |
|-------------------|----------|-----------------|--------------|
| Standard-ImageNet | 25%      | 60%             | 1.1m         |
| Standard-Reward   | 26%      | 62%             | 1.1m         |
| Dreaming (linear) | 39%      | 79%             | 1.4m         |
| Dreaming (conv)   | 62%      | 82%             | 1.8m         |
| Dreaming (TSD)    | 65%      | 92%             | 2.1m         |

### 6.3 Robot tasks and policy learning

Using our trained dreaming model, we are able to learn different policies entirely in the dreamed environment. We conduct the experiments with two different robot tasks. In one task, (i) we learn a policy to ‘approach the target object’,  $\pi_{ap}$ . We train a CNN,  $H(s_t)$  to output the binary classification if the given state is a goal state. For this task, our reward is -1 for all actions taken and +100 when the robot reaches the target. That is,  $R(s_t) = 100$  if  $H(s_t) > 0.5$  and -1 otherwise. This causes the agent to learn a policy to reach the target in as few steps as possible. In Fig. 3, we show an example dream sequence starting from a randomly sampled state.

Using the same dreaming model, (ii) we also learn a policy to ‘avoid the target’,  $\pi_{avoid}$ . Our reward function is  $\Delta v$  for each action and  $R(s_t) = -100$  when  $H(s_t) > 0.5$ . This makes the agent learn to move as much as possible, without hitting the target. Training details are described in Appendix A.

### 6.4 Offline evaluation

To evaluate various models and learned policies without running real-world robot trials, we collected a dataset consisting of image frames from the robot’s point of view, together with the ground truth geolocations of the robot and the target object. Given one image (from the real robot trajectory) as the start state, the task is to generate a dreamed trajectory from it by sequentially selecting actions following the learned policy while relying on the state-transition model. We ran this for 30 steps or until the goal detector CNN predicted the target had been reached. We then computed the distance between the ground truth location of the target object and the robot location after taking such  $\sim 30$  actions. If the distance is less than 20cm, we considered it a successful trial. Note that a successful trial happens only when both the dreaming model and the reinforcement policy learning on top of it are very accurate, since the state transitions have to happen  $\sim 30$  times.

Table 2 compares accuracies of several different reinforcement learning algorithms with baselines and dreaming models. We explicitly confirm that learning in a dream can be effectively done with various standard policy gradient algorithms (e.g., REINFORCE, Actor-Critic), and genetic algorithms (e.g., CMA-ES [11]). We find that starting from random states in addition to real states leads to a more accurate policy than starting only from real states (i.e., the previous methods), confirming that the ability to ‘dream’ is beneficial. We also compare to a baseline policy of constantly moving straight.

In Table 3 we compare the learned policies using Actor-Critic with baselines and dreaming models for both the target approach and the avoid tasks. To train these policies, we use both real and random starting states. We find that the standard state representation/transition model learning result in a constant policy. The linear representation trained with the decoder performs better, but not as well as our dreaming with convolutional representations. This confirms that maintaining the spatial

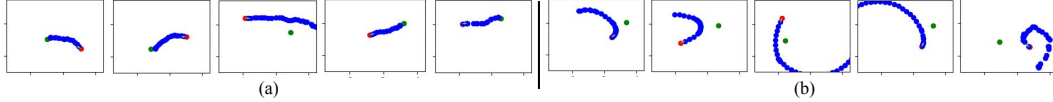


Figure 6: The red dot represents the robot’s starting location, the green dot is the target location, the blue dots are the resulting locations of the actions. On average, robot starts 2 meters away from the target. We show offline trajectories for the **(a)** approach task and **(b)** avoid task.

Table 4: Accuracies measured with real-world robot trials on both tasks. We tested 15 total trials split between 3 targets for each model in the approach task and 10 trials with 2 objects in the avoidance task. The target was on average 2.5 meters away from the robot for the approach target task and 0.6 meters away from the robot in the avoid task. We report the percentage of successful trials.

|                   | Seen Targets |       | Unseen Targets |       |
|-------------------|--------------|-------|----------------|-------|
|                   | Approach     | Avoid | Approach       | Avoid |
| Standard-Reward   | 0%           | 50%   | -              | -     |
| Dreaming (linear) | 27%          | 40%   | -              | -     |
| Dreaming (conv)   | 47%          | 100%  | 40%            | 20%   |
| Dreaming (TSD)    | 60%          | 100%  | 60%            | 90%   |

information is beneficial for policy learning. Additionally, we find that using a single encoder to learn a shared representation for all target objects provides the best results. Fig. 6 shows examples.

## 6.5 Real-world robot experiments

In Table 4, we compare the performances of the various models trained entirely in a dream and directly applied to the real-world setting. We demonstrate the ability to learn different policies in our two different tasks (i.e., approaching and avoiding), using a single state-transition model without any real-world robot trials. Actor-Critic was used as our reinforcement learning algorithm in this experiment. We are able to confirm that our dreaming model obtains better success rates on both tasks compared to the standard approach of using CNN states. Our convolutional dreaming showed a reasonable accuracy. Additionally, we conducted an experiment to approach/avoid an ‘unseen’ target. We find that using our TSD approach allowed the reinforcement learning agent to learn a general policy to successfully react to different targets. Fig. 7 shows a sequence of images the robot received during the approach task.

Once learned, our action policy CNN runs in real-time on a Nvidia Jetson TX2 mobile GPU.

## 7 Conclusion

We proposed the approach of learning real-world robot action policies by dreaming. The main idea is to learn a realistic dreaming model that can emulate samples equivalent to frame sequences from the real environment, and make the robot learn policies by interacting with the dreaming model instead of the real-world. We experimentally confirmed that we are able to learn a realistic dreaming model from a few initial random samples, and showed that the dreaming model together with a reinforcement learning algorithm enable learning of action policies directly applicable to real-world robots.

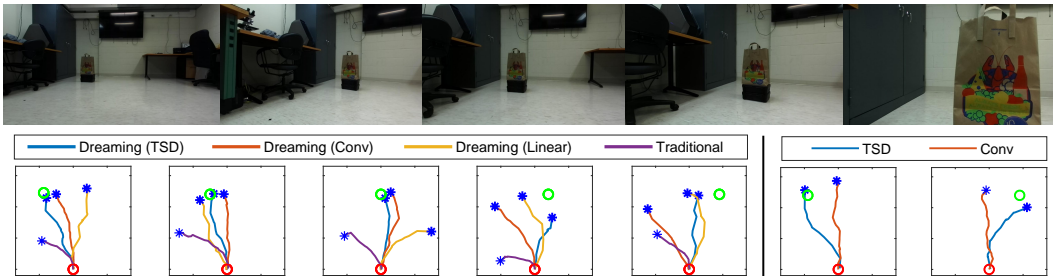


Figure 7: Example real-world robot frames (top), and trajectories of different models during the ‘approach’ task for seen (bottom left) and unseen (bottom right) targets.



## References

- [1] J. Carreira and A. Zisserman. Quo vadis, action recognition? a new model and the kinetics dataset. In *Proceedings of the IEEE Conference on Computer Vision and Pattern Recognition (CVPR)*, pages 4724–4733. IEEE, 2017.
- [2] P. Christiano, Z. Shah, I. Mordatch, J. Schneider, T. Blackwell, J. Tobin, P. Abbeel, and W. Zaremba. Transfer from simulation to real world through learning deep inverse dynamics model. *arXiv preprint arXiv:1610.03518*, 2016.
- [3] M. Deisenroth and C. E. Rasmussen. Pilco: A model-based and data-efficient approach to policy search. In *International Conference on Machine Learning (ICML)*, pages 465–472, 2011.
- [4] J. Deng, W. Dong, R. Socher, L.-J. Li, K. Li, and L. Fei-Fei. Imagenet: A large-scale hierarchical image database. In *Proceedings of the IEEE Conference on Computer Vision and Pattern Recognition (CVPR)*, pages 248–255. IEEE, 2009.
- [5] C. Finn, I. Goodfellow, and S. Levine. Unsupervised learning for physical interaction through video prediction. In *Advances in Neural Information Processing Systems (NIPS)*, pages 64–72, 2016.
- [6] C. Finn and S. Levine. Deep visual foresight for planning robot motion. In *IEEE International Conference on Robotics and Automation (ICRA)*. IEEE, 2017.
- [7] C. Finn, X. Y. Tan, Y. Duan, T. Darrell, S. Levine, and P. Abbeel. Deep spatial autoencoders for visuomotor learning. In *IEEE International Conference on Robotics and Automation (ICRA)*, pages 512–519. IEEE, 2016.
- [8] R. Girshick. Fast r-cnn. In *Proceedings of the IEEE International Conference on Computer Vision (ICCV)*, pages 1440–1448. IEEE, 2015.
- [9] S. Gu, T. Lillicrap, I. Sutskever, and S. Levine. Continuous deep q-learning with model-based acceleration. In *International Conference on Machine Learning (ICML)*, pages 2829–2838, 2016.
- [10] D. Ha and J. Schmidhuber. World models. *arXiv preprint arXiv:1803.10122*, 2018.
- [11] N. Hansen, S. D. Müller, and P. Koumoutsakos. Reducing the time complexity of the derandomized evolution strategy with covariance matrix adaptation (cma-es). *Evolutionary computation*, 11(1):1–18, 2003.
- [12] N. Heess, G. Wayne, D. Silver, T. Lillicrap, T. Erez, and Y. Tassa. Learning continuous control policies by stochastic value gradients. In *Advances in Neural Information Processing Systems (NIPS)*, pages 2944–2952, 2015.
- [13] D. P. Kingma and M. Welling. Auto-encoding variational bayes. *International Conference on Learning Representations (ICLR)*, 2014.
- [14] J. Koutník, J. Schmidhuber, and F. Gomez. Online evolution of deep convolutional network for vision-based reinforcement learning. In *International Conference on Simulation of Adaptive Behavior*, pages 260–269. Springer, 2014.
- [15] A. Krizhevsky, I. Sutskever, and G. E. Hinton. Imagenet classification with deep convolutional neural networks. In *Advances in Neural Information Processing Systems (NIPS)*, pages 1097–1105, 2012.
- [16] J. Lee and M. S. Ryoo. Learning robot activities from first-person human videos using convolutional future regression. In *IEEE/RSJ International Conference on Intelligent Robots and Systems (IROS)*, 2017.
- [17] I. Lenz, R. A. Knepper, and A. Saxena. Deepmpc: Learning deep latent features for model predictive control. In *Robotics: Science and Systems*, 2015.
- [18] S. Levine, P. Pastor, A. Krizhevsky, and D. Quillen. Learning hand-eye coordination for robotic grasping with deep learning and large-scale data collection. *arXiv preprint arXiv:1603.02199*, 2016.
- [19] W. Liu, D. Anguelov, D. Erhan, C. Szegedy, S. Reed, C.-Y. Fu, and A. C. Berg. Ssd: Single shot multibox detector. In *Proceedings of European Conference on Computer Vision (ECCV)*, pages 21–37. Springer, 2016.
- [20] R. McAllister and C. E. Rasmussen. Data-efficient reinforcement learning in continuous state-action gaussian-pomdps. In *Advances in Neural Information Processing Systems (NIPS)*, pages 2037–2046, 2017.
- [21] V. Mnih, K. Kavukcuoglu, D. Silver, A. Graves, I. Antonoglou, D. Wierstra, and M. Riedmiller. Playing atari with deep reinforcement learning. *arXiv preprint arXiv:1312.5602*, 2013.
- [22] A. Nagabandi, G. Kahn, R. S. Fearing, and S. Levine. Neural network dynamics for model-based deep reinforcement learning with model-free fine-tuning. *arXiv preprint arXiv:1708.02596*, 2017.
- [23] J. Oh, S. Singh, and H. Lee. Value prediction network. *Advances in Neural Information Processing Systems (NIPS)*, 2017.
- [24] A. Piergiovanni and M. S. Ryoo. Learning latent super-events to detect multiple activities in videos. *Proceedings of the IEEE Conference on Computer Vision and Pattern Recognition (CVPR)*, 2018.
- [25] L. Pinto and A. Gupta. Supersizing self-supervision: Learning to grasp from 50k tries and 700 robot hours. In *IEEE International Conference on Robotics and Automation (ICRA)*, pages 3406–3413. IEEE, 2016.
- [26] V. Pong, S. Gu, M. Dalal, and S. Levine. Temporal difference models: Model-free deep rl for model-based control. *arXiv preprint arXiv:1802.09081*, 2018.
- [27] D. Silver, H. van Hasselt, M. Hessel, T. Schaul, A. Guez, T. Harley, G. Dulac-Arnold, D. Reichert, N. Rabinowitz, A. Barreto, et al. The predictor: End-to-end learning and planning. *International Conference on Machine Learning (ICML)*, 2016.
- [28] K. Simonyan and A. Zisserman. Very deep convolutional networks for large-scale image recognition. *arXiv preprint arXiv:1409.1556*, 2014.
- [29] R. S. Sutton. Integrated architectures for learning, planning, and reacting based on approximating dynamic programming. In *Machine Learning Proceedings 1990*, pages 216–224. Elsevier, 1990.

- [30] M. E. Taylor and P. Stone. Transfer learning for reinforcement learning domains: A survey. *Journal of Machine Learning Research*, 10(Jul):1633–1685, 2009.
- [31] J. Tobin, R. Fong, A. Ray, J. Schneider, W. Zaremba, and P. Abbeel. Domain randomization for transferring deep neural networks from simulation to the real world. In *IEEE/RSJ International Conference on Intelligent Robots and Systems (IROS)*, 2017.
- [32] E. Tzeng, C. Devin, J. Hoffman, C. Finn, X. Peng, S. Levine, K. Saenko, and T. Darrell. Towards adapting deep visuomotor representations from simulated to real environments. *arXiv preprint arXiv:1511.07111*, 2015.
- [33] A. Venkatraman, R. Capobianco, L. Pinto, M. Hebert, D. Nardi, and J. A. Bagnell. Improved learning of dynamics models for control. In *International Symposium on Experimental Robotics*, pages 703–713. Springer, 2016.
- [34] N. Wahlström, T. B. Schön, and M. P. Deisenroth. From pixels to torques: Policy learning with deep dynamical models. *arXiv preprint arXiv:1502.02251*, 2015.
- [35] M. Watter, J. Springenberg, J. Boedecker, and M. Riedmiller. Embed to control: A locally linear latent dynamics model for control from raw images. In *Advances in Neural Information Processing Systems (NIPS)*, 2015.
- [36] T. Weber, S. Racanière, D. P. Reichert, L. Buesing, A. Guez, D. J. Rezende, A. P. Badia, O. Vinyals, N. Heess, Y. Li, et al. Imagination-augmented agents for deep reinforcement learning. *Advances in Neural Information Processing Systems (NIPS)*, 2017.
- [37] F. Zhang, J. Leitner, M. Milford, B. Upcroft, and P. Corke. Towards vision-based deep reinforcement learning for robotic motion control. *arXiv preprint arXiv:1511.03791*, 2015.

## A Implementation details

### A.1 Model architectures

We implement our models in PyTorch. Our convolutional autoencoder takes images of size  $64 \times 64$  as input. The encoder network has 4 convolutional layers, all with kernel size  $4 \times 4$  with a stride of 2, no padding and followed by a ReLU activation function. The layers have 32, 64, 128, and 256 channels. We then have two  $1 \times 1$  convolutional layers with no activation function. These layers produce  $\mu$  and  $\sigma$  used to obtain the latent representation. This results in a  $2 \times 2 \times 256$  dimensional state representation

The decoder network starts with a convolutional layer with 256 channels and a  $3 \times 3$  kernel, stride of 1 and padding of 1 followed by a ReLU activation function. The decoder then has 5 transposed convolutional layers (also called deconvolutional layers) with kernel size  $4 \times 4$  and upsampled by a factor of 2. The layers have 128, 64, 32, and 3 channels. This results in the output being a  $64 \times 64$  image.

The action representation network has 2 fully connected layers, going from 3 to 64 to 128. Since our actions can be negative, we use the LeakyReLU activation function:

$$\text{LeakyReLU}(x) \begin{cases} -0.2x & x \leq 0 \\ x & 0 \geq 0 \end{cases} \quad (6)$$

The 256-dimensional vector is reshaped into a  $2 \times 2 \times 32$  tensor. This is used as input to a convolutional layer with a  $3 \times 3$  kernel with 32 channels, stride of 1 and padding of 1, followed by the LeakyReLU function. The next layer is a  $1 \times 1$  convolutional layer with 64 channels followed by the LeakyReLU.

The output of the action representation network is concatenated with the state representation giving a  $2 \times 2 \times 256 + 64$  dimensional representation. This is used as input to the future regression (or state-transition) CNN. This CNN consists of 4 convolutional layers, each followed by the LeakyReLU function. The first layer has 512 channels, a  $3 \times 3$  kernel with stride of 1 and padding of 1. The second has 512 channels,  $1 \times 1$  kernel, a stride of 1 and no padding. The third layer has 256 channels a  $3 \times 3$  kernel and padding of 1. The final layer has 256 channels and a  $1 \times 1$  kernel.

The reward/end detector CNN has 2 convolutional layers. The first is  $2 \times 2$  with 32 channels, followed by a ReLU activation function and the second is  $1 \times 1$  with 1 channel followed by a sigmoid activation function. This network predicts the probability of a given  $2 \times 2 \times 256$  state representation being the goal.

The actor/policy network have the same architecture regardless of reinforcement learning algorithm. They consist of a convolutional layer with a  $2 \times 2$  kernel, ReLU, convolutional with  $1 \times 1$  and 3 channels. This produces the action. The critic follows the same architecture, except the final layer has 1 output channel.

### A.2 Training details

**Dreaming model:** We jointly train the autoencoder and future regressor with the Adam method. We set the learning rate to 0.001 for 20 epochs. After every 10 epochs, we decay the learning rate by a factor of 10.

**Reinforcement learning:** To train the actor-critic and REINFORCE networks, for each iteration we use a batch of 256 trajectories run up to 30 steps. These trajectories are obtained from our dreaming model and was not from the real-world environment; we are able to generate as many trajectories as we want for any policy as needed. Note that this takes very little time to execute as only the future regressor and reward CNNs run all on a GPU. We use the Adam method with the learning rate set to 0.01 for 2000 iterations.

To train policies with CMA-ES, we uses a population size of 128. For each candidate network, we used a batch of 256 trajectories and ran each for up to 30 steps. We computed the mean reward for the batch and followed the CMA-ES algorithm to generate the next candidate networks. We ran CMA-ES for 50 iterations.

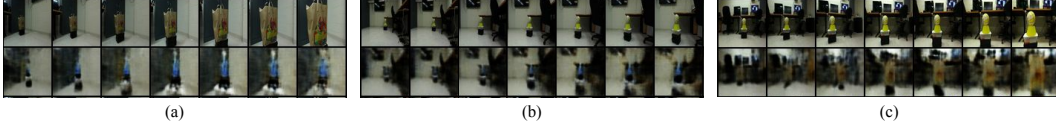


Figure 8: Example sequence of target transfer. (a) A sequence of an unseen bag transferred into a bottle. (b) An unseen volleyball transferred into a bottle. (c) An unseen volleyball turned into a bag.

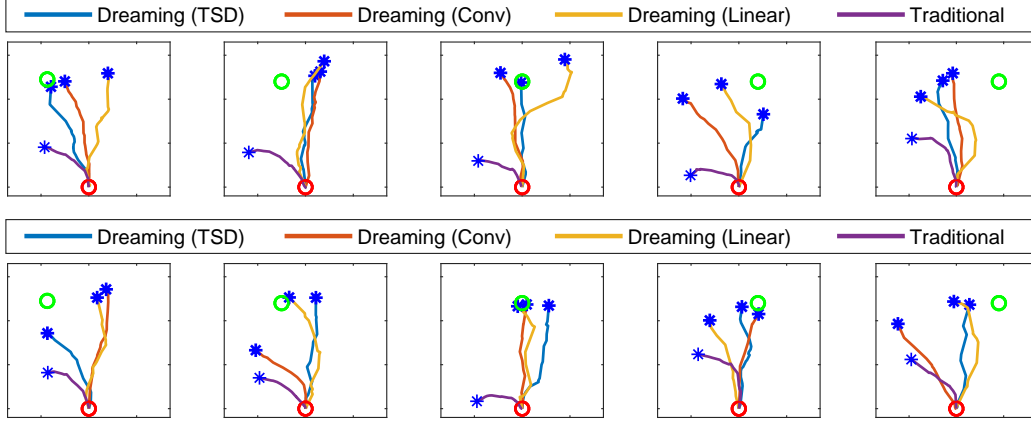


Figure 9: Trajectories on the approaching task taken by the robot in the real world for various different seen targets. The target was on average 2.5 meters away from the robot.

## B Additional examples

In Fig 8, we show three example sequences of the target transfers. The model is given input of an image containing an unseen target. Applying one of the target-specific decoders produces an image with the other target.

In Fig. 9, we show example real-world robot trajectories for approaching seen targets. In Fig. 10, we shown example real-world trajectories for approaching unseen targets. In Fig. 13, we show an example trajectory annotated with the robot's point of view.

In Fig. 11, we show several real-world robot trajectories for avoiding a seen target. In Fig. 12, we show several example trajectories for avoiding an unseen target.

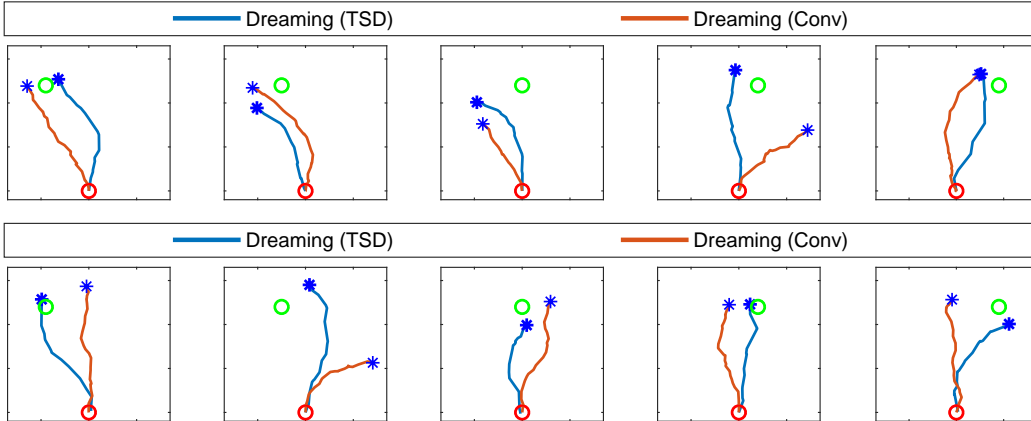


Figure 10: Trajectories on the approaching task taken by the robot in the real world for unseen targets.

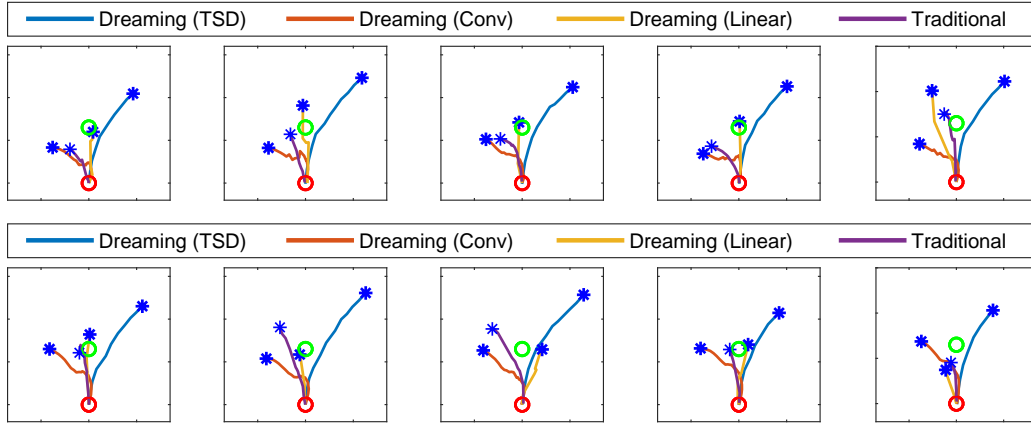


Figure 11: Trajectories on the avoiding task taken by the robot in the real world for various seen targets. To make this task more challenging, the target was placed on average 0.6 meters away from the robot.

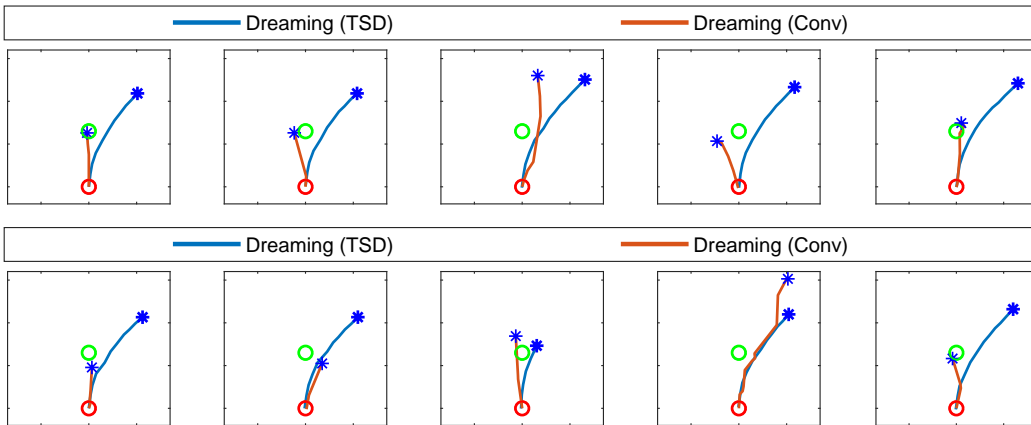


Figure 12: Trajectories on the avoiding task taken by the robot in the real world for unseen targets. To make this task more challenging, the target was placed on average 0.6 meters away from the robot.

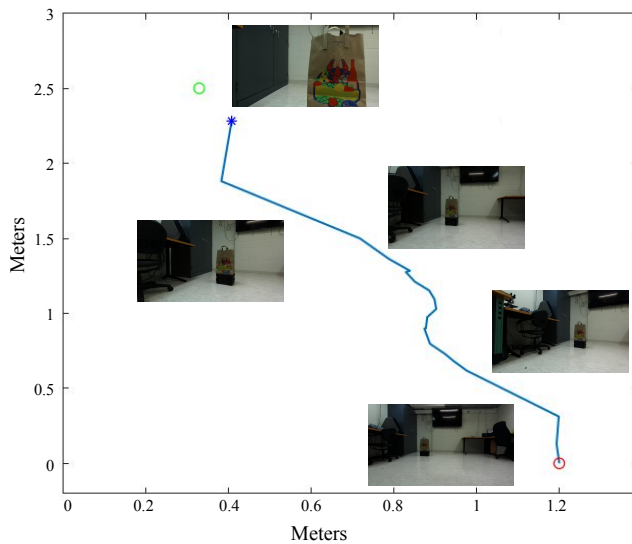


Figure 13: A real-world trajectory annotated with the robot's point of view.